



**HAL**  
open science

# Flight Demonstration Testing with Distributed Optical Fiber Sensor

Nozomi Saito, Takashi Yari, Kiyoshi Enomoto

► **To cite this version:**

Nozomi Saito, Takashi Yari, Kiyoshi Enomoto. Flight Demonstration Testing with Distributed Optical Fiber Sensor. EWSHM - 7th European Workshop on Structural Health Monitoring, IFFSTTAR, Inria, Université de Nantes, Jul 2014, Nantes, France. hal-01020354

**HAL Id: hal-01020354**

**<https://inria.hal.science/hal-01020354>**

Submitted on 8 Jul 2014

**HAL** is a multi-disciplinary open access archive for the deposit and dissemination of scientific research documents, whether they are published or not. The documents may come from teaching and research institutions in France or abroad, or from public or private research centers.

L'archive ouverte pluridisciplinaire **HAL**, est destinée au dépôt et à la diffusion de documents scientifiques de niveau recherche, publiés ou non, émanant des établissements d'enseignement et de recherche français ou étrangers, des laboratoires publics ou privés.

## FLIGHT DEMONSTRATION TESTING WITH DISTRIBUTED OPTICAL FIBER SENSOR

Nozomi Saito<sup>1</sup>, Takashi Yari<sup>1</sup>, Kiyoshi Enomoto<sup>2</sup>

<sup>1</sup>Mitsubishi Heavy Industries, Ltd., Structural Mechanics Research Laboratory,  
Nagoya Research & Development Center, Technology & Innovation Headquarters,  
10, Oye-cho, Minato-ku, Nagoya-city, Aichi, 455-8515 Japan

<sup>2</sup>SOKEIZAI Center, Kikai Shinko Bldg #301-3, 3-5-8, Shibakoen, Minato-ku, Tokyo, 105-0011  
Japan  
nozomi\_saito@mhi.co.jp

### ABSTRACT

This paper reports flight demonstration test results using an airborne structural health monitoring system with distributed optical fiber sensor. The test was conducted using a business jet in order to verify operability and feasibility of the airborne monitoring system. An optical fiber sensor was attached on the front spar of the vertical tail and the measurement device was on the cabin floor of the business jet. Dynamic strain and temperature changes during flights were measured and those values were close to those measured by strain gages and a thermocouple. Static distributed strain and temperature changes during flights were also measured and those values denoted the same tendency to those measured by the strain gages and the thermocouple. Despite the good results, there were some errors on temperature measurement results. The authors, therefore, developed a new installation method to decrease the temperature measurement errors. These developments mean that the operability and feasibility of our monitoring system in actual flights were verified.

**KEYWORDS :** *Optical fiber sensor, Brillouin scattering, flight test, strain, temperature.*

### INTRODUCTION

Structural health monitoring (SHM) significantly contributes to reducing maintenance costs, improving flight safety and fuel efficiency [1]. Maintenance scheme change from conventional schedule-based to condition-based will significantly contribute to reduce maintenance costs. Condition-based maintenance (CBM) means that hidden area inspection will be conducted only when SHM system indicates presence of structural damages without disassembly and reassembly. Fast damage detection by real-time monitoring during flights and reduction of human errors during inspections will be effective to improving flight safety. Furthermore, innovative structural design on the premise of SHM will achieve structural weight saving and thus fuel efficiency. Therefore many aircraft and system manufactures are conducting their own SHM research and development (R&D) programs. In these R&D programs, many kinds of sensors are utilized such as piezoelectric materials [2], comparative vacuum monitoring (CVM) technology [3] and optical fiber sensors [4].

Optical fiber sensor (OFS), which is one of SHM technologies developed in the world, has great characteristics such as light weight, high electromagnetic durability and capability to be embedded into composites. While there are many optical fiber SHM technologies in the world, the authors are developing the Brillouin optical correlation domain analysis (BOCDA)[5] because the BOCDA has more superior characteristics than the other OFS technologies for wide-area monitoring as shown in table 1. In table 1, BGS (Brillouin Gain Spectrum) and DGS (Dynamic Gain Spectrum) are BOCDA measurement results mainly affects strain and temperature measurement values, respectively. The most important characteristic of the BOCDA is distributed strain and temperature sensing with high spatial resolution. Second is dynamic strain and

temperature sensing at arbitrary points in an OFS. Thirdly, the BOCDA measures strain and temperature simultaneously in an OFS with polarization maintaining property utilizing the Brillouin scattering and birefringence phenomena[6]. In this paper, OFS means the OFS with this property.

Application scenarios of the BOCDA-SHM system are distributed sensing along an OFS and real-time dynamic sensing at arbitrary points during flights. In distributed sensing, structural damages will be detected by measuring distributed strain changes. In real-time dynamic sensing, not only structural damages will be detected, but fatigue life will be also predicted. Fig. 1 shows the application scenarios of the system. The authors have been raised the technology readiness level (TRL)[7] of the BOCDA-SHM system in order to realize these scenarios. The prototype of BOCDA device has been already manufactured on trial[8], durability evaluation of the system involving attached sensors and measurement devices, probability of detection (PoD) evaluation have been also conducted[9-11]. These developments established the TRL of the system is approximately 6.

This paper reports the flight demonstration test results from among developments previously mentioned. Flight demonstration test was conducted in order to verify operability and feasibility of the BOCDA-SHM system using an attached OFS and a prototype airborne device which measures strain and temperature simultaneously. A business jet, MU-300, was used as the test bed. An OFS was attached on the front spar of the vertical tail and devices were on the cabin floor of the jet. Dynamic strain changes during ascending, descending and right-left turning flights were measured and those values were close to those measured by strain gages. However, there were some errors on temperature measurements by BOCDA compared with temperature measured by a thermocouple. The authors, therefore, developed an improved OFS installation method in order to decrease the temperature measurement errors. Strain and temperature distributions measured by BOCDA during steady bank flights denoted the same tendency of those measured by the strain gages and the thermocouple.

Table 1: Characteristics of BOCDA

Characteristics	Values	Unit
Measurement range	1000	m
Spatial resolution of BGS	1.6	mm
Spatial resolution of DGS	100	mm
Sampling rate	1000	Hz

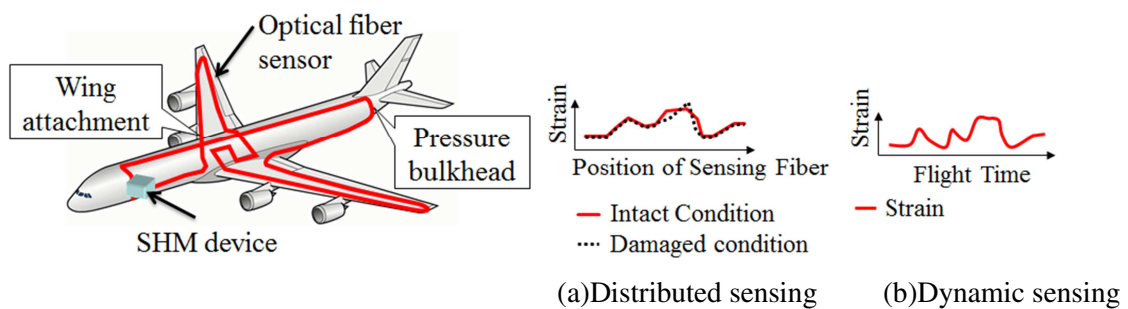


Figure 1: Application scenario of BOCDA-SHM system

## 1 MEASUREMENT PRINCIPLE

The BOCDA is based on a stimulated Brillouin scattering (SBS) and birefringence phenomena in an OFS. Because the two parameters are physically independent, this method ensures a complete discrimination of strain and temperature. SBS occurs when two light waves, the pump light and the probe light, counter-propagate inside an OFS, and the probe light frequency is lower than the pump light frequency by  $\nu_B$  called as the Brillouin frequency shift (BFS). Its spectrum is called the Brillouin gain spectrum (BGS). When an axial strain is loaded to an OFS, density fluctuations occur in an OFS. This fluctuation changes the speed of the acoustic wave, and the speed change of the acoustic wave make the BFS changes, that is, the strain changes of an OFS. The BOCDA measurement principle is shown in Figure 2. The temperature changes are obtained from  $f_{yx}$  called as the central frequency deviation of the dynamic grating spectrum (DGS) generated in the SBS process. Strain and temperature changes ( $\Delta\varepsilon$  and  $\Delta T$ ) are calculated on Equation (1):

$$\begin{pmatrix} \Delta\varepsilon \\ \Delta T \end{pmatrix} = \frac{1}{C_v^\varepsilon \cdot C_f^T - C_v^T \cdot C_f^\varepsilon} \begin{pmatrix} C_f^T & -C_v^T \\ -C_f^\varepsilon & C_v^\varepsilon \end{pmatrix} \begin{pmatrix} \Delta\nu_B \\ \Delta f_{yx} \end{pmatrix} \quad (1)$$

$C_v^\varepsilon$  and  $C_v^T$  are coefficients of  $\nu_B$ , which affect to strain and temperature, respectively.  $C_f^\varepsilon$  and  $C_f^T$  are coefficients of  $f_{yx}$ , which affect to strain and temperature, respectively. These coefficients, which were evaluated in tensile strain and temperature loaded test, are presented on Equation (2):

$$\begin{aligned} C_v^\varepsilon &= 4.98 \times 10^{-2} \text{ MHz}/\mu\varepsilon \\ C_v^T &= 1.02 \text{ MHz}/^\circ\text{C} \\ C_f^\varepsilon &= 1.03 \text{ MHz}/\mu\varepsilon \\ C_f^T &= -62.3 \text{ MHz}/^\circ\text{C} \end{aligned} \quad (2)$$

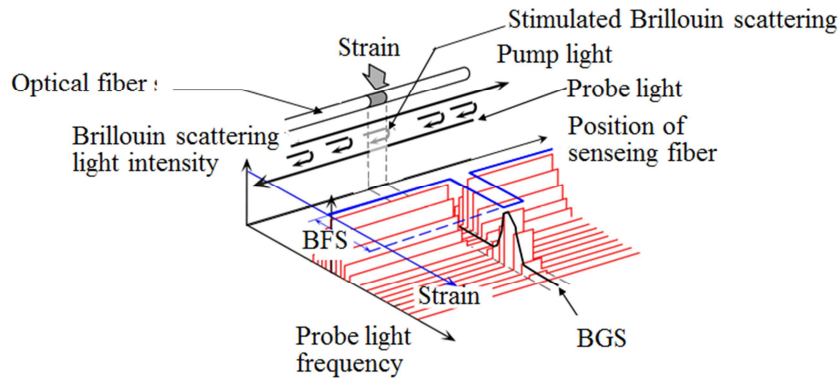


Figure 2: Measurement principle of BOCDA

## 2 FLIGHT DEMONSTRATION TEST

### 2.1 Test Bed

Test bed in the flight demonstration test was an eleven-seated business jet, MU-300, which was produced by Mitsubishi heavy industries, LTD. Its length and width are 14.7 m and 13.7 m, respectively. An OFS was attached on the front spar of the vertical tail using epoxy based adhesive. The clad diameter of the OFS used in the test was 125  $\mu\text{m}$ . Strain gages and a thermocouple were also attached near the OFS for reference. The OFS and lead wires of the strain gages and the thermocouple were through the pressure bulkhead, then connected to the measuring devices on the cabin. Figure 3 shows the test bed in the flight demonstration test.

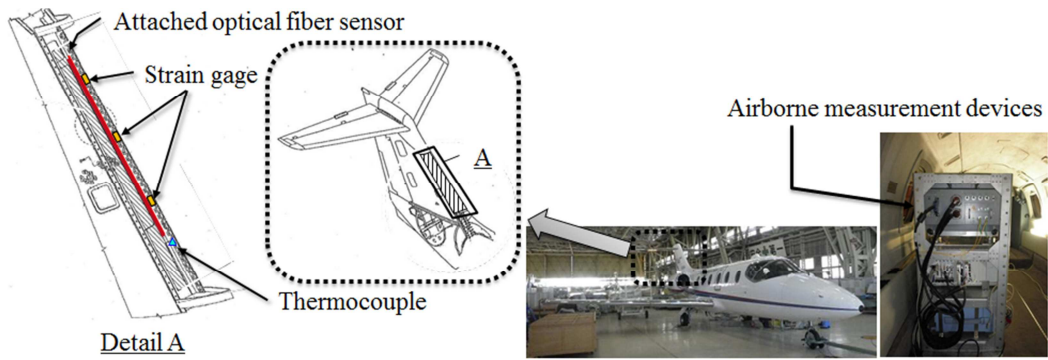


Figure 3: Test bed in flight demonstration test

### 2.2 Test Procedures

The BOCDA measured dynamic strain and temperature changes near legacy sensors (strain gages and a thermocouple) during take-off and ascending, right-left turning flights and descending. Strain and temperature distributions changes were measured during level flights and steady bank flights. Spatial resolutions of BGS and DGS in the test were 30 mm and 300 mm, respectively. Sampling rates were 1.6 Hz at strain-temperature simultaneous measurement and 27.8 Hz at strain measurement.

### 2.3 Results and Discussions

Figure 4 shows dynamic strain and temperature measurement results during take-off and ascending. Although, from take-off to about 700 sec., temperature and strain changes measured by the BOCDA were close to reference values by legacy measurements, there were errors on strain and temperature between measured by BOCDA and legacy measurements after about 700 sec. The cause of these errors was considered that the coefficients related to the birefringence phenomena might be different from the coefficients shown in equation (2) when OFS was compressed. The authors, therefore, conducted four-point bending tests in order to investigate the cause of these errors.

Figure 5 and Figure 6 show test results during right-left turning flights, measuring strain and temperature simultaneously and measuring only strain, respectively. Strain change measured by the BOCDA was close to that measured by the strain gages. Temperature changes shown in Figure 5, however, have some errors. This was also because of the coefficient differences in strain-temperature discrimination equation when OFS was compressed and tensioned.

Figure 7 shows distributed strain and temperature changes during the steady bank flight. Strain and temperature distributions measured by BOCDA denoted the same tendency to the reference values by legacy measurements. The values of strain and temperature did not coincide with the reference values. The reason why there were the margins of these values was that actual strain and temperature changes from during level flight were too small compared with measurement accuracies of the BOCDA device in this measurements, which were  $\pm 50 \mu\epsilon$  and  $\pm 2^\circ\text{C}$ .

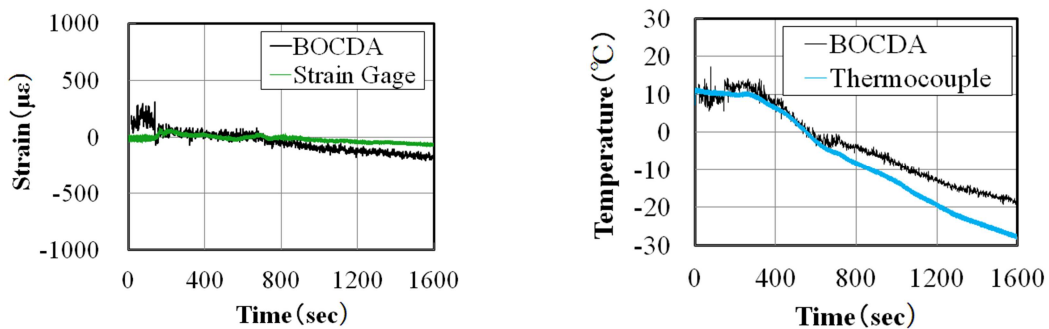


Figure 4: Dynamic strain and temperature changes during take-off and ascending

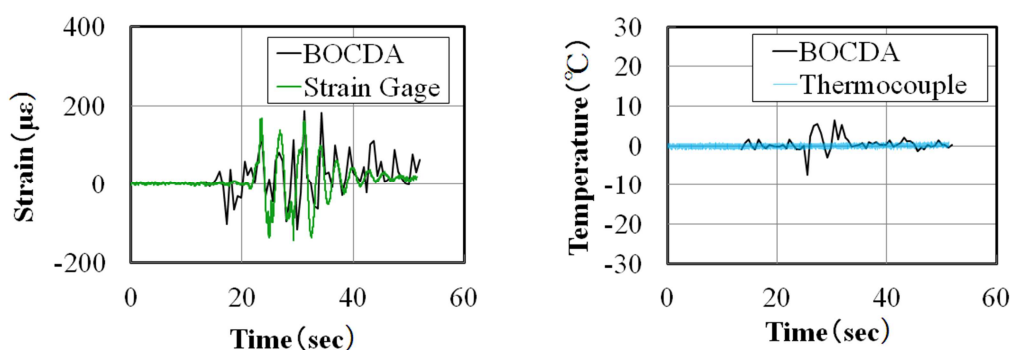


Figure 5: Dynamic strain and temperature changes during right-left turning flights

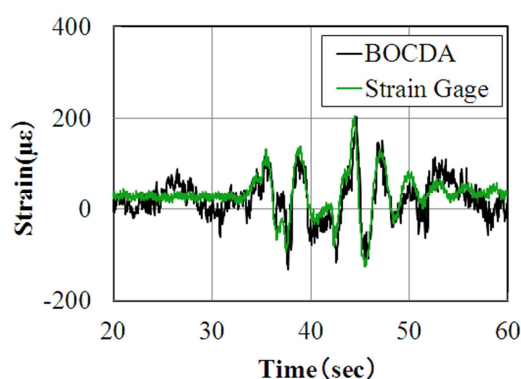


Figure 6: Dynamic strain changes during right-left turning flights

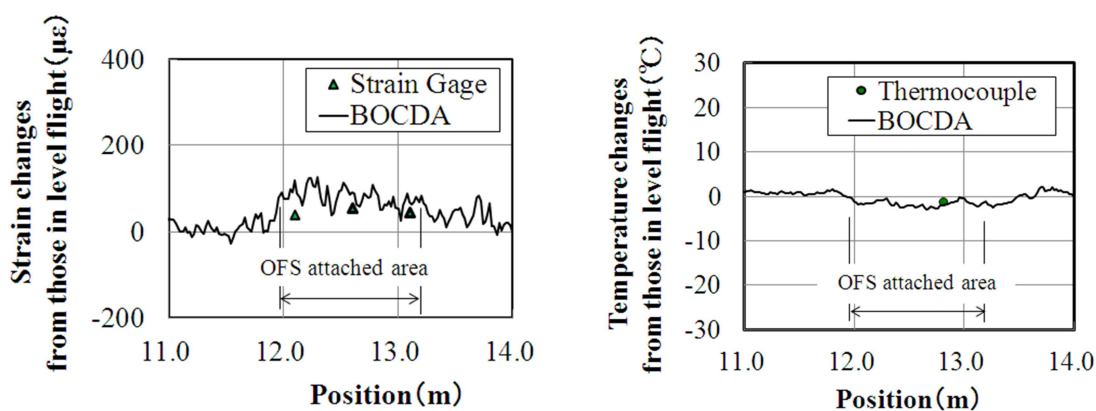


Figure 7: Distributed strain and temperature changes during steady banking flights

### 3 CAUSES OF ERRORS IN TEMPERATURE MEASUREMENT

In order to investigate the causes of errors in BOCDA temperature measurements and to propose a new OFS installation method avoiding these errors, four-point bending tests were conducted using Al plates with attached OFSs, strain gages and a thermocouple. BOCDA measured temperature at each strain status and temperature values were more different compared with those measured by the thermocouple as OFS compression strain increased. The authors, therefore, assumed that the coefficients shown in equation (2) might be different when OFS was compressed and also proposed a new OFS installation method to decrease these temperature measurement errors.

### 3.1 Four-point bending test

Four-point bending tests were conducted using Al plates with attached OFSs, strain gages and a thermocouple. Figure 8 and figure 9 show a test specimen and test set-up in the four-point bending tests. One of the attached OFSs was attached with no pre-strain and the other was attached with pre-tensile strain, which was about 3000  $\mu\epsilon$ .

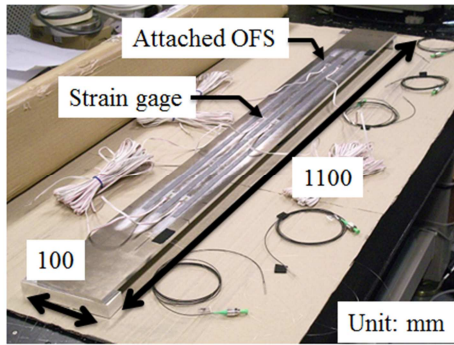


Figure 8: Test specimen

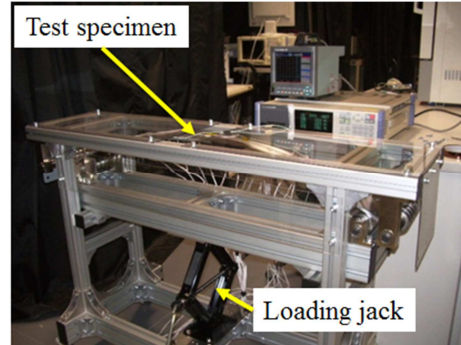


Figure 9: Test set-up

### 3.2 Results and Discussions

Figure 10 shows the temperature measurement results in the tests using no pre-strained OFS(a) and pre-tensile strained OFS(b). Temperature measured by BOCDA with pre-tensile strained OFS was close to that measured by the thermocouple while temperature measured by BOCDA with no pre-strained OFS has larger error as OFS compression strain increased. This means that coefficients shown in equation (2) might be adapted only when OFS was tensioned and might be different when OFS was compressed. The cause of temperature measurement error in the flight demonstration tests was that the strain-temperature discrimination coefficients adaptable only when OFS was tensioned were adapted even when OFS was compressed.

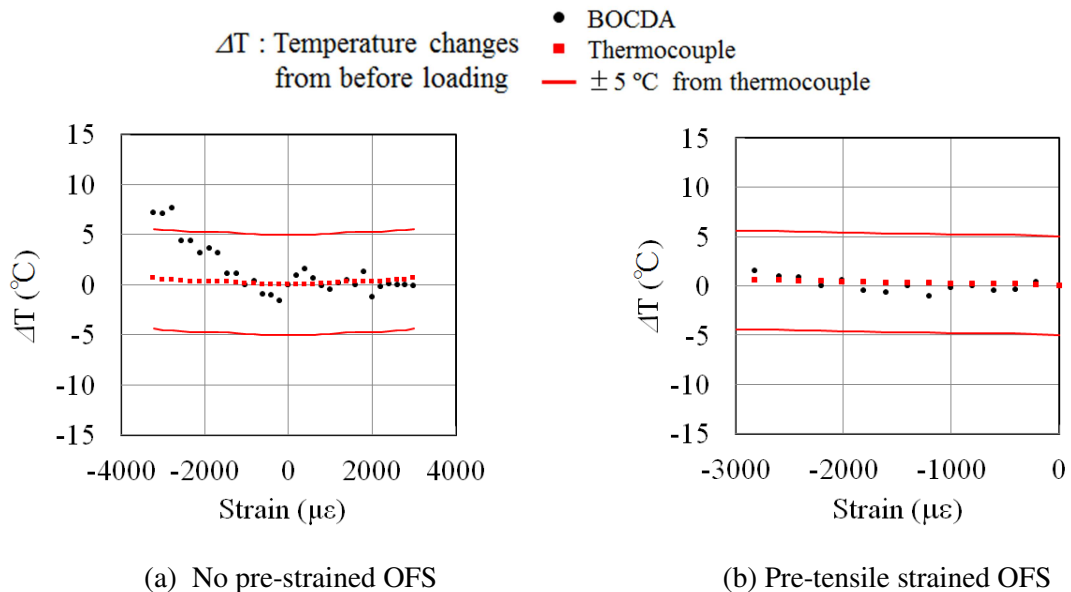


Figure 10: Temperature measurement results

## CONCLUSION

This paper reports the flight demonstration test results. Flight demonstration test was conducted to verify operability and feasibility of the airborne BOCDA-SHM device. Strain and temperature changes during flights were monitored simultaneously with the BOCDA-SHM system. Temperature measurement results with the system had some errors compared with temperature measured by a thermocouple. Therefore, four-point bending test was conducted to investigate the cause of these measurement errors. Temperature changes were measured by BOCDA when OFS was tensioned and compressed in the four-point bending test. To decrease temperature measurement errors, the authors propose a new OFS installation method, pre-tensioned installation method. The conclusions of this study are summarized as followings.

- Strain changes measured by the airborne BOCDA-SHM device were close to these values measured by the strain gages in the flight test. Although there were some errors on temperature in compression strain region, operability and feasibility of the airborne device were verified.
- Temperature measurement errors in compression region were able to decrease by pre-tensioned OFS installation method.

## ACKNOWLEDGEMENT

This work was conducted as a part of the project, “Advanced Materials & Process Development for Next-Generation Aircraft Structures” under the contract with SOKEIZAI Center, founded by Ministry of Economy, Trade and Industry (METI) of Japan.

## REFERENCES

- [1] D. Roach, S. Neidigk, Does the Maturity of Structural Health Monitoring Technology Match User Readiness?, *Proceedings of the 8th International Workshop on Structural Health Monitoring*, 1:39-52, 2011.
- [2] N. Salowitz, Z. Guo, S. Roy, R. Nardari, Y. H. Li, S. J. Kim, F. Kopsaftopoulos, F. K. Chang, A Vision on Stretchable Bio-Inspired Networks for Intelligent Structures, *Proceedings of the 9th International Workshop on Structural Health Monitoring*, 1:35-44, 2013.
- [3] M. Wishaw, D. P. Barton, Comparative Vacuum Monitoring: a New Method of In-Situ Real-Time Crack Detection and Monitoring, *Proceedings of the Symposium – International Committee on Aeronautical Fatigue*, 657-666, 2002.
- [4] A. Othonos, K. Kalli, Fiber Bragg Gratings: *Fundamentals and Applications in Telecommunications and Sensing*, Norwood, Artech House Publishers, 1999.
- [5] K. Y. Song, Z. He, K. Hotate, Distributed Strain Measurement with Millimeter-order Spatial Resolution based on Brillouin Optical Correlation Domain Analysis, *OSA Optics letters*, 31, 17:2526-2528, 2006.
- [6] W. Zou, Z. He, K. Hotate, Demonstration of Brillouin Distributed Discrimination of Strain and Temperature Using a Polarization -Maintaining Optical Fiber, *IEEE Photonics Technology Letters*, 22, 8:526-528, 2010.
- [7] J. C. Mankins, Technology Readiness Levels, *a white paper*, 1995.
- [8] T. Yari, M. Ishioka, K. Nagai, M. Ibaragi, K. Hotate, Y. Koshioka, Monitoring Aircraft Structural Health Using Optical Fiber Sensors, *Mitsubishi Heavy Industries Technical Review*, 45, 4:5-8, 2008.
- [9] T. Yari, N. Saito, K. Nagai, K. Hotate, K. Enomoto, the Development of BOCDA-SHM System for Reduction of Airplane Operation Costs, *Mitsubishi Heavy Industries Technical Review*, 48, 4:75-79, 2011.
- [10] N. Saito, T. Yari, K. Hotate, M. Kishi, S. Matsuura, K. Kumagai, K. Enomoto, Developmental Status of SHM Applications for Aircraft Structures Using Distributed Optical Fiber, *Proceedings of the 9th International Workshop on Structural Health Monitoring*, 1:2011-2018, 2013.

- [11] Y. Kumagai, S. Matsuura, T. Yari, N. Saito, K. Hotate, M. Kishi, M. Yoshida, Fiber-optic Distributed Strain and Temperature Sensor using BOCDA Technology at High Speed and with High Spatial Resolution – Taking on Aircraft Structural Health Monitoring -, *Yokogawa Technical Report*, 56, 2:81-84, 2013.